

Electronic Supplementary Information for

Precipitation of Er³⁺-doped Na₅Y₉F₃₂ Crystals from Fluoro-phosphate Glasses: An Advanced Solid-state NMR Spectroscopic Study

Xuyang Zhang,^{ab} Ruili Zhang,^c Lili Hu,^{ab} Jinjun Ren^{*ab}

Fluorine Quantification

Due to the high-temperature evaporation of fluoride material, the final residual fluorine content in glass must be different from the nominal content. We estimate the precise fluorine quantities by means of ¹⁹F rotor-synchronized Hahn spin echo NMR method, using BaF₂ as an internal quantification standard. Spin echo NMR method rather than single-pulse method was used to obtain better baselines for the quantification. Considering the effect of T₂ relaxation, two individual experiments were conducted for each sample with the evolution time of one and two rotor periods, respectively. In addition, since the relaxation delay of BaF₂ crystal is too long (500 s), the relaxation delay of 32 s for glass samples was used in the following quantification experiments. Each glass sample and BaF₂ standard were mixed with the nominal F⁻ molar ratio of 4:1. Fig. S1 (a) shows the ¹⁹F MAS NMR spectra of BaF₂ at the relaxation delays of 32 and 500 s, respectively. Fig. S1 (b) shows the representative quantification results of 16BaF₂-72NaPO₃-12YF₃ glass. The resonance of the BaF₂ standard added to the sample is well separated at -14.6 ppm from that of the glass. The spectra were fitted to Gauss/Lorentz curves, using the DMFIT package.¹

The intensity I_0 is obtained from I_1 (one rotor period) and I_2 (two rotor periods) as follows:

$$I_0/I_1 = I_1/I_2 = f$$

Thus, the intensity

$$I_0 = I_1 \times f$$

Considering the effect of relaxation delay,

$$I_{\text{BaF}_2} = I_0(\text{BaF}_2) \times (I_{500\text{s}}/I_{32\text{s}})$$

Here, $I_{500\text{s}}$ and $I_{32\text{s}}$ are obtained from single-pulse experiments, as shown in Fig. S1 (a).

Therefore, the ratio of (residual F content)/(nominal F content) denoted as F_r could be obtained as follows:

$$F_r = (I_{\text{Ba-F}\dots\text{Na}} \times f_{\text{Ba-F}\dots\text{Na}} + I_{\text{P-F}\dots\text{Na}} \times f_{\text{P-F}\dots\text{Na}} + I_{\text{Y-F}\dots\text{Na}} \times f_{\text{Y-F}\dots\text{Na}}) / I_{\text{BaF}_2} \times 4 = 20.4\%$$

^a Key Laboratory of Materials for High Power Laser, Shanghai Institute of Optics and Fine Mechanics, Chinese Academy of Sciences, Shanghai 201800, P. R. China

*Email: renjinjunsiom@163.com

^b Center of Materials Science and Optoelectronics Engineering, University of Chinese Academy of Sciences, Beijing 100049, China

^c School of Material Science and Engineering, University of Jinan, Jinan, 250022, P. R. China

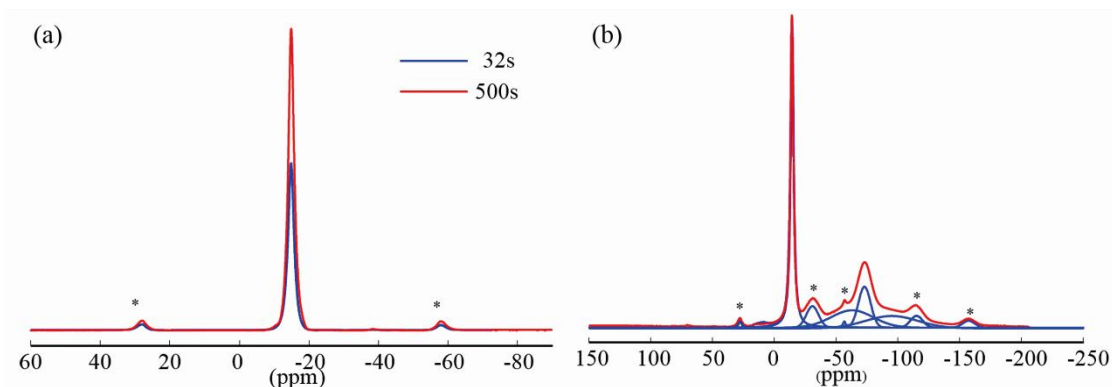


Fig. S1 (a) ^{19}F MAS NMR spectra of BaF_2 at the relaxation delays of 32 and 500 s, respectively. (b) ^{19}F rotor-synchronized Hahn spin echo NMR spectra of $16\text{BaF}_2\text{-}72\text{NaPO}_3\text{-}12\text{YF}_3$ glass and BaF_2 standard with the nominal F⁻ molar ratio of 4:1. Line shape deconvolution components are displayed by solid blue curves, and their sum is displayed as the red curve. Spinning sidebands are indicated by asterisks.

Phosphorous Quantification

Quantitative phosphorous contents were determined by a ^{31}P single-pulse solid state NMR procedure, using AlP_3O_9 as an internal quantification standard. Considering the tremendous relaxation time of AlP_3O_9 crystal (5120 s), the relaxation time of glasses (160 s) was used in the phosphorous quantification experiment. Two spectra acquired at different relaxation time of 160 s and 5120 s was compared to calibrate the effect of relaxation delay of AlP_3O_9 crystal. The results are shown in Fig. S2 (a). Fig. S2 (b) shows the representative quantification results of $16\text{BaF}_2\text{-}48\text{NaPO}_3\text{-}36\text{YF}_3$ glass. The signal of the AlP_3O_9 crystal locating at -50.6 ppm is well separated from that of the glass. By comparing the integration intensity of the spectra including the sidebands, the analyzed P content can be obtained.

The intensity of AlP_3O_9 crystal was calibrated as follows:

$$I_{\text{AlP}_3\text{O}_9} = I_{0(\text{AlP}_3\text{O}_9)} \times (I_{5120\text{s}}/I_{160\text{s}})$$

Where $I_{5120\text{s}}$ and $I_{160\text{s}}$ are the integrated spectrum intensity of AlP_3O_9 crystal obtained at the relaxation of 5120 s and 160 s, respectively, from single-pulse experiments, as shown in Fig. S2 (a).

Therefore, the ratio of (residual P content)/(nominal P content) denoted as P_r could be obtained as follows:

$$P_r = I_{\text{glass}}/I_{\text{AlP}_3\text{O}_9} = 117.2\%$$

Where I_{glass} is the integration intensity of glass spectra.

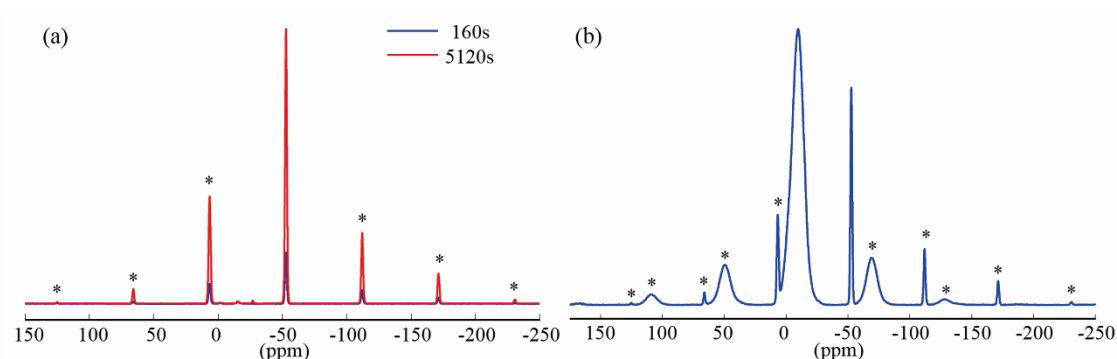


Fig. S2 (a) ^{31}P MAS NMR spectra of AlP_3O_9 acquired at the relaxation delays of 160 and 5120 s, respectively. (b) ^{31}P MAS NMR spectra of $16\text{BaF}_2\text{-}48\text{NaPO}_3\text{-}36\text{YF}_3$ glass mixed with AlP_3O_9 standard with the nominal P^{5+} molar ratio of 1:1. Spinning sidebands are indicated by asterisks.

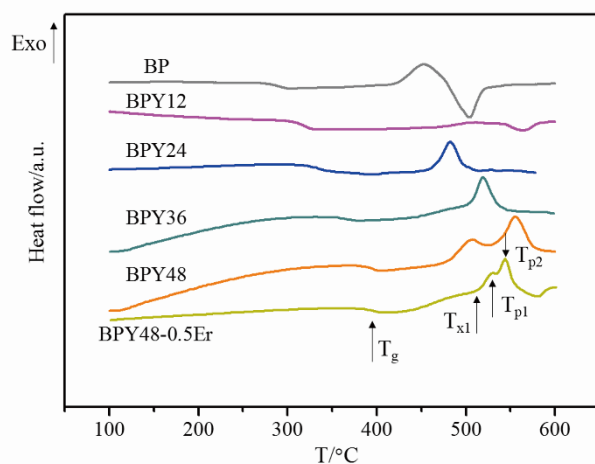


Fig. S3 DSC curves of BPYx glasses and BPY48–0.5Er glass.

Table S1 The characteristic temperatures of the samples. T_g , glass transition temperature, T_x , the onset crystallization temperature, T_{p1} , the first maximum crystallization temperature, T_{p2} , the second maximum crystallization temperature

Samples	$T_g/^\circ\text{C}$ ($\pm 5^\circ\text{C}$)	$T_x/^\circ\text{C}$ ($\pm 5^\circ\text{C}$)	$T_{p1}/^\circ\text{C}$ ($\pm 5^\circ\text{C}$)	$T_{p2}/^\circ\text{C}$ ($\pm 5^\circ\text{C}$)	$T_x - T_g/^\circ\text{C}$ ($\pm 5^\circ\text{C}$)
BP	285				
BPY12	312				
BPY24	322	450	480		128
BPY36	350	490	518		140
BPY48	399	478	507	555	79
BPY48-0.5Er	397	503	527	542	106

Table S2 Raman scattering maxima observed in BPYx glasses and corresponding peak assignments

Samples	Vibrational mode	Wave number (cm^{-1})
BP	$(\text{P-O-P})_{\text{sym}}$ modes of long chain	690
	$(\text{PO}_3)_{\text{sym}}$	1010
	$(\text{PO}_2)_{\text{sym}}$	1150
BPY12	$(\text{P-O-P})_{\text{sym}}$ modes of long chain	715
	$(\text{PO}_3)_{\text{sym}}$	1026
	$(\text{PO}_2)_{\text{sym}}$	1126
BPY24	$(\text{P-O-P})_{\text{sym}}$ modes of short chain	739
	$(\text{PO}_3)_{\text{sym}}$	1039
	$(\text{PO}_2)_{\text{sym}}$	1110
BPY36	$(\text{P-O-P})_{\text{sym}}$ modes of short chain	746
	$(\text{PO}_4)_{\text{sym}}$	960
	$(\text{PO}_3)_{\text{sym}}$	1044
BPY48	$(\text{P-O-P})_{\text{sym}}$ modes of short chain	750
	$(\text{PO}_4)_{\text{sym}}$	965
	$(\text{PO}_3)_{\text{sym}}$	1048

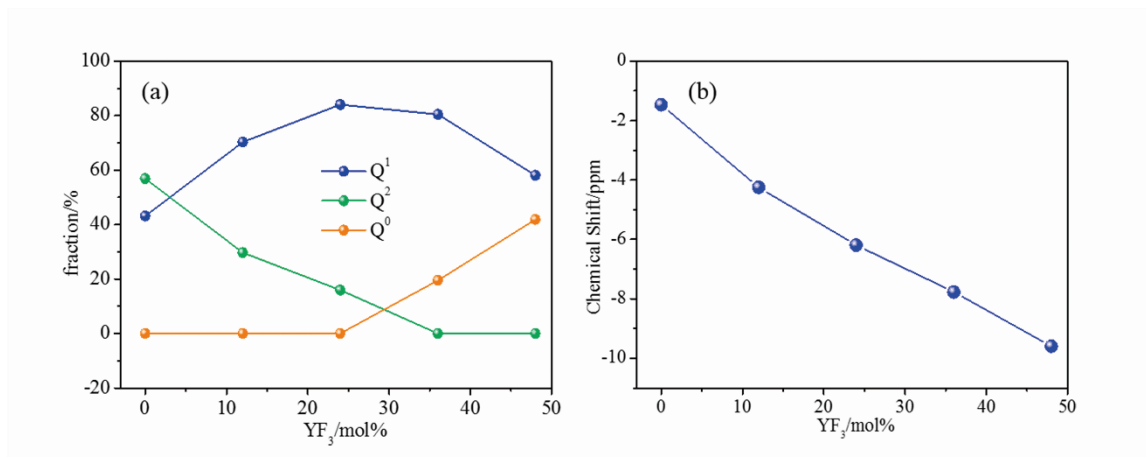


Fig. S4 (a) The evolution of various Qⁿ units with YF₃ content. (b) The evolution of chemical shift of Q¹ units with YF₃ content.

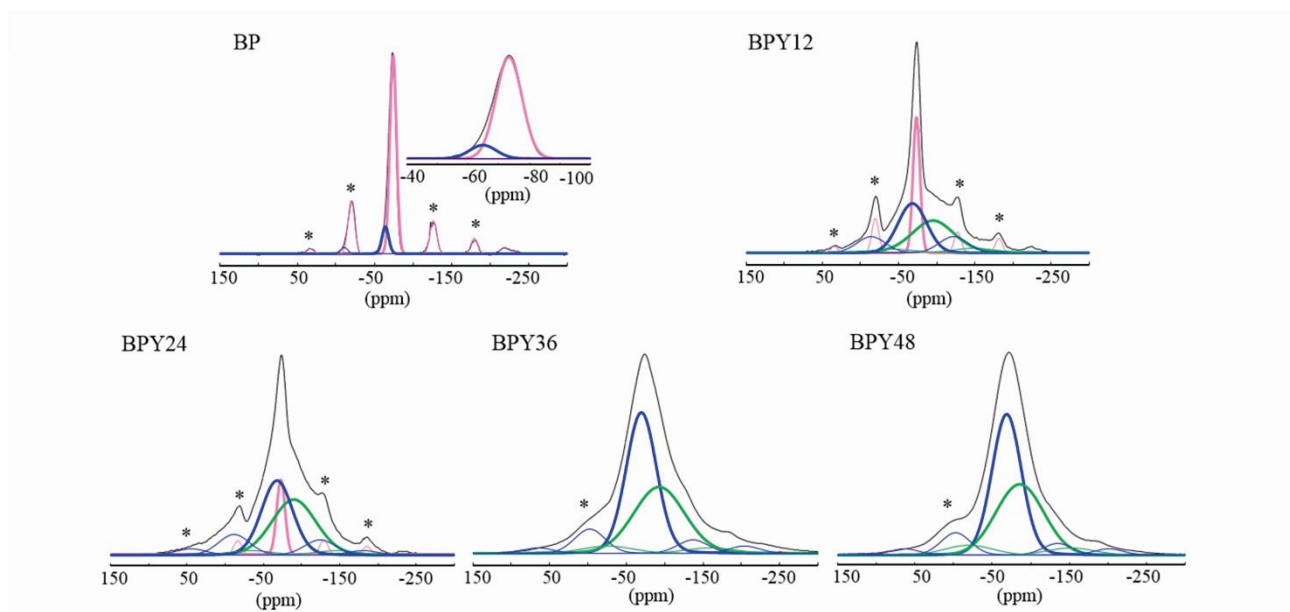


Fig. S5 Deconvolution of the ¹⁹F MAS NMR spectra of BPY_x glasses. The pink, blue, and green solid lines represent ¹⁹F in P-F...Na, Ba-F...Na, and Y-F...Na, respectively. All the spinning sidebands are illustrated by thin lines and denoted by asterisks.

Table S3 Deconvolution of the ¹⁹F MAS NMR spectra of all the glasses studied

Samples		δ_{CS}^{iso} (ppm) (± 0.3 ppm)	<i>FWHM</i> (ppm) (± 0.3 ppm)	Fraction (%) ($\pm 2\%$)
BP	Ba-F...Na	-65.0	10.2	11.9
	P-F...Na	-73.5	10.0	88.1
BPY12	Ba-F...Na	-68.0	44.0	41.1
	P-F...Na	-73.5	10.8	26.0
	Y-F...Na	-95.0	65.1	32.9
BPY24	Ba-F...Na	-68.2	48.0	50.2
	P-F...Na	-73.5	12.8	12.0
	Y-F...Na	-90.2	68.0	37.8
BPY36	Ba-F...Na	-69.8	47.0	59.4
	Y-F...Na	-93.2	78.44	40.6
BPY48	Ba-F...Na	-69.1	45.1	57.7
	Y-F...Na	-86.8	73.2	42.3

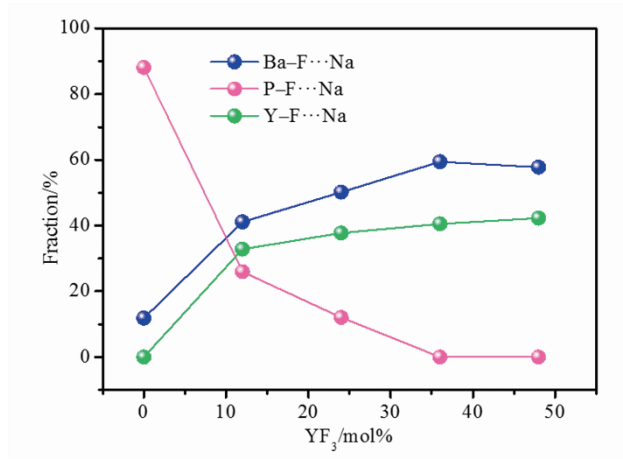


Fig. S6 The evolution of various F species with YF₃ content.

¹⁹F static Hahn spin echo NMR results

Fig. S7 summarizes the results of ¹⁹F static Hahn spin echo decay measurements of BPY24 and BPY48 glasses. The ¹⁹F decay spectra of BPY24 and BPY48 glasses acquired at different evolution times are shown in part (a) and (b), respectively. Part (c) shows the Gaussian fitting of the spin echo amplitudes according to the expression:

$$I_{(2t_1)}/I_0 = \exp\{-(2t_1)^2 M_2^{F-F}/2\}$$

which has been confirmed experimentally in its application to glass system. In this expression, M_2^{F-F} denotes the homonuclear dipolar second moment, characterizing the ¹⁹F-¹⁹F magnetic dipole-dipole interactions. The obtained M_2^{F-F} values are summarized in Table 5. It is not unexpected that the M_2^{F-F} value of BPY48 glass ($1267 \times 10^6 \text{ rad}^2 \text{ s}^{-2}$) is larger than that of BPY24 glass ($527 \times 10^6 \text{ rad}^2 \text{ s}^{-2}$).

The M_2^{F-F} values can also be calculated based on the distance between the F ions using the following equations:²

$$M_2^{F-F} = 3/5 (\mu_0/4\pi)^2 I(I+1) \gamma^4 \hbar^2 N^{-1} \sum d_{ij}^{-6} \quad (\text{a})$$

$$M_2^{F-F} = 4/15 (\mu_0/4\pi)^2 I(I+1) \gamma^4 \hbar^2 N^{-1} \sum d_{ij}^{-6} \quad (\text{b})$$

where γ is the gyromagnetic ratio of the nucleus, I is the spin quantum number, and N is the number of nuclei involved. When the spectra are dominated by the homogeneous broadening, equation (a) is appropriate. When the spectra are dominated by inhomogeneous broadening, equation (b) is appropriate. For glasses, equation (b) is appropriate due to their disorder structures. In order to simply compare the concentration of F⁻ ions in glasses with that in NaYF₄ crystals, we also take the equation (b) to calculate the theoretical M_2^{F-F} values based on the crystal structure files.

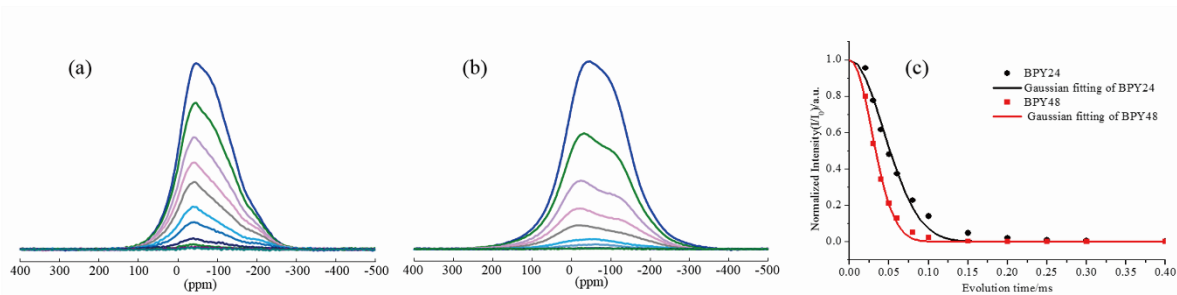


Fig. S7 ¹⁹F static Hahn spin echo spectra of representative BPY24 (a) and BPY48 (b) glasses at different evolution times (20, 30, 40, 50, 60, 80, 100, 150, 200, 250, 300, and 400 μs , respectively). (c) ¹⁹F static Hahn spin echo amplitudes of BPY24 and BPY48 glasses as a function of dipolar evolution times. All the experimental data are obtained by integrating the whole spectra. The solids curves represent the fitting results of the data using Gaussian function within the short term range of $2t_1 \leq 60 \mu\text{s}$, yielding the M_2^{F-F} values listed in Table 5.

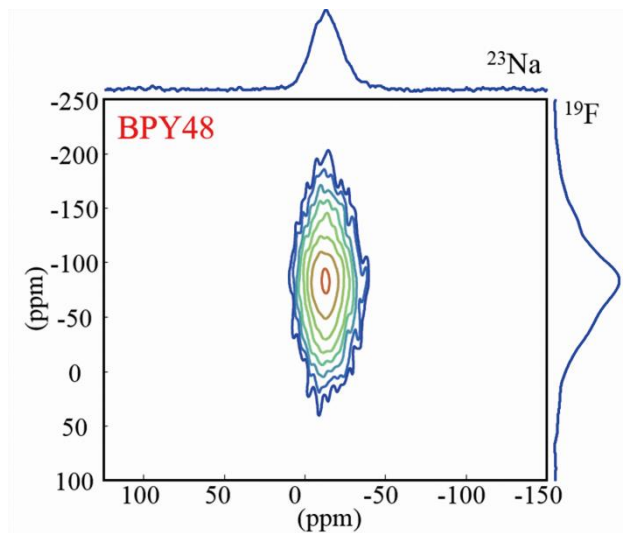


Fig. S8 ^{23}Na $\{^{19}\text{F}\}$ HETCOR spectrum of BPY48 sample.

NMR results of paramagnetic Er^{3+} doped glasses

The ^{19}F , ^{31}P , and ^{23}Na MAS NMR spectra of ErF_3 -doped samples are shown in Fig. S9. Apparently, the spinning sidebands of ^{19}F spectra are enhanced with the increase in ErF_3 content (Fig. S9 (a)), originating from the dipolar couplings between the ^{19}F spins and the unpaired electron spins of the Er^{3+} ions. This observation indicates that Er^{3+} ions are increasingly in close proximity to F⁻ ions with the increase in Er^{3+} ion concentration. The ^{31}P and ^{23}Na spectra gradually broaden simultaneously due to the paramagnetic effects of Er^{3+} ions (Fig. S9 (b) and (c)). Fig. S10 exhibits the relationships between ErF_3 content and the peak width of ^{31}P spectra. This plot reveals a roughly linear increase in the peak width with increasing ErF_3 content, indicating a random distribution of Er^{3+} ions around P groups and no formation of clusters.

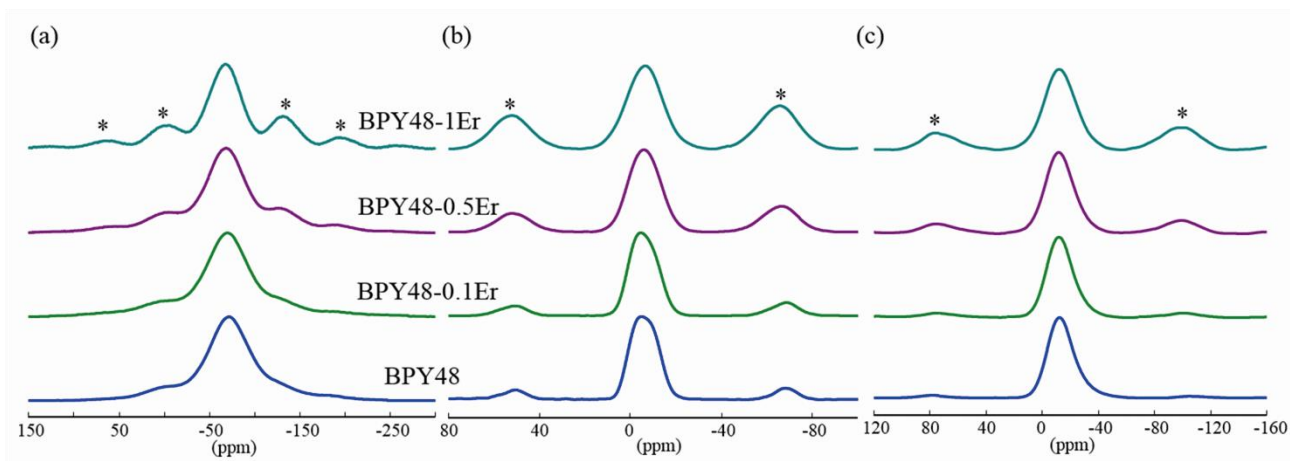


Fig. S9 (a) ^{19}F MAS NMR spectra of Er^{3+} -doped glasses. (b) ^{31}P MAS NMR spectra of Er^{3+} -doped glasses. (c) ^{23}Na MAS NMR spectra of Er^{3+} -doped glasses.

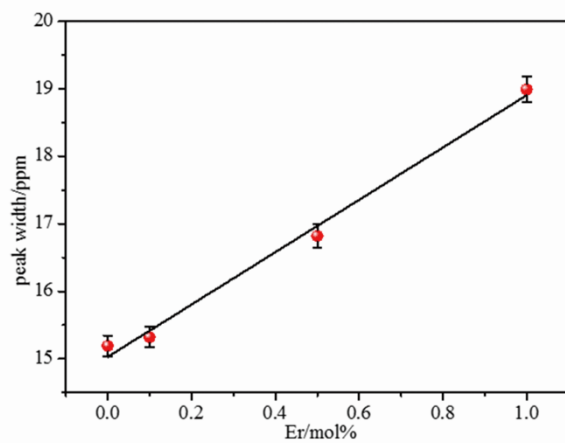


Fig. S10 The evolution of peak width of ^{31}P MAS spectra with Er^{3+} doping.

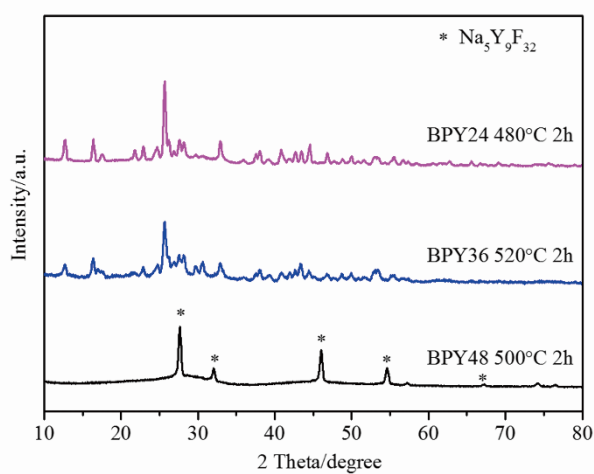


Fig. S11 The XRD patterns of BPY24 glass heated at 480°C for 2 h, BPY36 glass heated at 520°C for 2 h, and BPY48 glass heated at 500°C for 2 h.

Table S4 Heated treatment conditions for the glass samples

Samples	Different temperature	Different time at 490°C
BPY24	540°C 2 h	
BPY36	520°C 2 h	
BPY48 and BPY48-0.5Er	480°C 2 h	0.5 h
	490°C 2 h	1 h
	500°C 2 h	1.5 h
	510°C 2 h	2 h

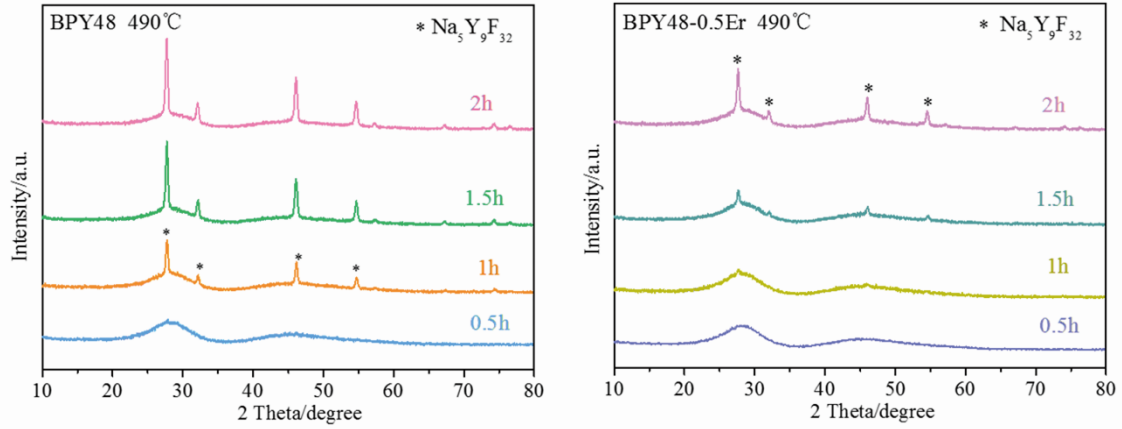


Fig. S12 XRD patterns of BPY48 and BPY48–0.5Er samples heat treated at 490°C for different periods of time (0.5 h, 1 h, 1.5 h, 2 h).

Table S5 Peak deconvolution results of BPY48 glass and glass ceramic heated at 490°C for 2h

Samples	δ_{CS}^{iso} (ppm) (± 0.3 ppm)	<i>FWHM</i> (ppm) (± 0.3 ppm)	Fraction (%) ($\pm 2\%$)	
BPY48	Q ⁰	-2.1	9.3	46.1
	Q ¹	-9.5	10.2	53.9
BPY48 490°C 2h	Q ⁰	-2.3	9.3	44.2
	Q ¹	-9.2	10.3	55.8

References

1. D. Massiot, F. Fayon, M. Capron, I. King, S. Le Calve, B. Alonso, J. O. Durand, B. Bujoli, Z. H. Gan and G. Hoatson, *Magn. Reson. Chem.*, 2002, **40**, 70-76.
2. D. Lathrop and H. Eckert, *J. Am. Chem. Soc.*, 1989, **111**, 3536-3541.